

# Factors influencing the major ion chemistry in the Tihama coastal plain of southern Saudi Arabia: evidences from hydrochemical facies analyses and ionic relationships

Faisal K. Zaidi<sup>1</sup> · Abdulaziz M. Al-Bassam<sup>1</sup> · Osama M. K. Kassem<sup>1,2</sup> · Hussain J. Alfaifi<sup>1</sup> · Saad M. Alhumidan<sup>1</sup>

Received: 6 February 2017 / Accepted: 6 July 2017 / Published online: 11 July 2017  
© Springer-Verlag GmbH Germany 2017

**Abstract** Coastal aquifers across the globe have been a subject of extensive research mainly because of problems related to saline water intrusion as a consequence of global climate changes and overabstraction of groundwater. The present work deals with the assessment of factors which affects the groundwater chemistry in parts of the Tihama coastal plains in the Jazan Province of southern Saudi Arabia. Hydrochemical parameters (pH, EC, TDS, major ions, NO<sub>3</sub> and SiO<sub>2</sub>) were obtained from 263 wells and were interpreted. Hydrochemical facies analyses revealed two main types of groundwater facies, i.e., the mixed groundwater facies predominantly confined to the eastern and central part of the study area (away from the coast) and groundwater facies dominated by SO<sub>4</sub> + Cl + NO<sub>3</sub> ions found mostly in the coastal zones in the western part of the study area. The average TDS value of the mixed groundwater facies is 945.7 mg/l, whereas the average TDS value is 3149.7 mg/l for the SO<sub>4</sub> + Cl + NO<sub>3</sub> anionic species. Greater influence of rainfall recharge can be observed in the mixed-water species, while saline water mixing or rock–water interaction can be seen in the SO<sub>4</sub>–Cl–NO<sub>3</sub> type of anionic species. However, ionic ratios point more toward rock–water interaction rather than saline water mixing in the groundwater facies dominated by SO<sub>4</sub>–Cl–NO<sub>3</sub> ions. This interpretation is also supported by the presence of sabkhas (salt flats) in the coastal zones where its interaction with the groundwater has resulted in high Cl

and SO<sub>4</sub> concentration. Cl/Br ratios which have often been used to detect saline water intrusion in coastal zones also do not support saline water intrusion in the study area. Ionic ratios point toward dissolution and base ion exchange as the main factors influencing the groundwater chemistry. Silicate weathering and silica dissolution are also found in the area. Saturation indices point toward gypsum and halite dissolution. The average NO<sub>3</sub> concentration is 157.80 mg/l and is mostly attributed to the agricultural practices in the region. The presence of shallow unconfined aquifers facilitate the easy percolation of irrigation return flows enriched in NO<sub>3</sub> concentration from the application of inorganic fertilizers on the agricultural farms.

**Keywords** Tihama coastal plain · Jazan Province · Hydrochemical facies · Silicate weathering

## Introduction

Coastal areas across the globe have been associated with ever-increasing population pressure and socioeconomic activities (Sekovski et al. 2012). One of the main reasons for the population pressure in these zones is the availability of shallow groundwater resources under unconfined conditions. These coastal aquifers have been the home and source for freshwater to more than one billion people across the globe (Small and Nicholls 2003). However, people inhabiting the coastal areas are also exposed to environmental hazards which mainly include saline water intrusion due to rise in sea levels or due to the overabstraction of groundwater (Taylor et al. 2013). The mixing of seawater with the fresh groundwater impairs the groundwater usage for domestic or agricultural purposes there by leading to water stress. Therefore, an

✉ Faisal K. Zaidi  
fzaidi@ksu.edu.sa

<sup>1</sup> SGSRC, Geology and Geophysics Department, College of Science, King Saud University, Riyadh, Saudi Arabia

<sup>2</sup> Department of Geology, National Research Center, Al-Behoos Street, Dokki, Cairo 12622, Egypt

understanding of the groundwater chemistry and the potential sources of contamination are important in coastal areas especially in arid regions as they are under constant pressure from population growth, higher per capita groundwater consumption and intense agricultural activities (El Alfy et al. 2015).

Keeping in view the significance of coastal aquifers, the present study was carried out in the Tihama coastal plain in southern Saudi Arabia. The study area is a part of the Jazan Province. The area has been investigated by numerous workers and includes the studies such as the groundwater characteristics and pollution assessment (El Alfy et al. 2015), aquifer delineation using geoelectric methods (Mogren et al. 2011), assessment of groundwater quality with respect to domestic and agricultural usage (Batayneh et al. 2012), saline water intrusion assessment using tracers (Abdalla 2016), saline water assessment using geoelectric and hydrochemical methods (Al-Bassam and Hussein 2008) and groundwater resource assessment (Abdalla et al. 2015). Abdalla (2016) point toward the phenomenon of saline water intrusion and do not take into consideration the influence of groundwater interaction with the sabkha deposits present in the region which might be responsible for the high groundwater salinity in the coastal zones. El Alfy et al. (2015) primarily use the geostatistical techniques to assess the main factors impacting groundwater. The other studies are based on geophysical investigations to conclude the presence of saline water intrusion in the area. The present study focuses on classical hydrochemical interpretation including facies analysis, ionic relationships and saturation indices of the major ions to understand the factors influencing the overall groundwater chemistry of the region. Cl/Br ratios have also been investigated in this study to see the possible influence of saline water intrusion.

### Study area description

The study area lies between the latitudes 16.39° and 17.225°N and longitudes 42.4° and 43.265°E and is a part of the Jazan Province of Saudi Arabia (Fig. 1). Geomorphologically the area can be divided into two main units: (a) the Tihama coastal plains in the west and (b) the Hijaz–Asir highlands in the east. The two geomorphological units are separated from each other by an escarpment which runs parallel to the Red Sea coast. Sabkhas are the other minor features which are found along the coasts. The climate of the area is hot and arid with temperatures ranging from more than 40 °C in summers to about 20 °C in winters. The rainfall in the region is characterized by large spatiotemporal variations and ranges from 100 mm/year in the coastal plains to about 400 mm/year in the eastern highlands (Subyani 2004; NCAO 2008). The elevation ranges

from 1538 m in the Hijaz–Asir highlands to 0 m along the coast (Fig. 1).

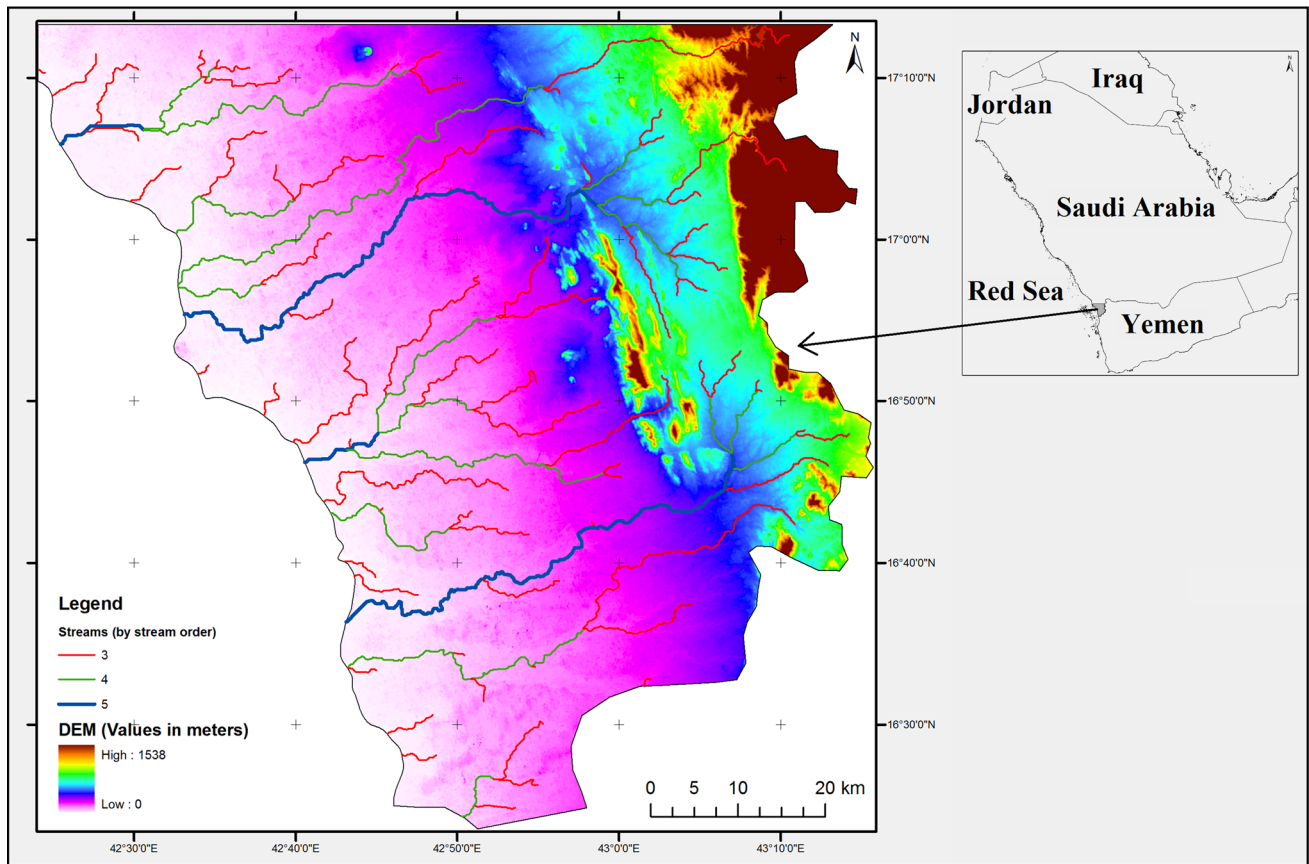
### Geology

Figure 2 shows the geological map of the study area. Geologically, the study area can be divided into two distinct geological units: the eastern part comprising of the Proterozoic basement rocks and the western part comprising of the quaternary deposits of the Tihama coastal plains. The Proterozoic basement rocks consist of metavolcanics, metaclastics, metaplutonics and metasediments (Fairer 1983). The Paleozoic succession is represented by the Cambro–Ordovician Wahid sandstone which unconformably overlies the Proterozoic basement (Dabbagh and Rogers 1983). The Mesozoic succession in the area occurs in the form of the Jurassic Khums and Arman formation which unconformably overlies the basement rocks.

The Cenozoic magmatic rocks occur in the form of Oligocene to Miocene Tihama–Asir magmatic complex and the quaternary basalts. Bulk of the Cenozoic succession is represented by the Quaternary sediments comprising of alternating layers of sand and gravel derived mainly from the weathering of the basement rocks in the Hijaz–Asir highlands. These quaternary deposits form the main aquifer system of the study area. The evolution of the Red Sea basin has resulted in the accumulation of salts along the entire coastal area and forms the sabkha deposits (salt flats) dominated by the presence of halite and gypsum (El Alfy et al. 2015).

### Hydrogeology

Shallow weathered aquifer in the Proterozoic basement rocks and the alluvial aquifers along the coastal plains are the main aquifer system in the study area. Groundwater in the wadi alluvium occurs in the unconfined state. These alluvial aquifers are the main source of water for domestic, agricultural and industrial usage in the study area. Water level measurements from 120 wells drilled in the wadi alluvium ranges from 5 m to 49.6 m below ground level. Geoelectric measurements have shown an increasing saturated thickness of the aquifer from the highlands in the eastern part of the study area toward the coast (Hussein and Ibrahim 1997; Al-Bassam and Hussein 2008). Figure 3 shows the piezometric level which varies from 89.3 to 1.15 m and flows toward the coast. However, several undulations can be seen in the piezometric contours close to the coast. These contour patterns are influenced by the groundwater pumping in the region mostly for agricultural activities. The main source of groundwater in the region is from precipitation which occurs mainly in the winter season. The coastal soils with its sandy texture have high



**Fig. 1** Location and DEM of the study area

infiltration rates which facilitates rainfall recharge (Abdalla et al. 2015). Hydrogeological investigations in parts of the Tihama coastal plain have shown that the transmissivity values range from 144 to 5760 m<sup>2</sup>/day (Al-Ahmadi and El-Fiky 2009).

**Methodology**

The water table measurement data and hydrochemical data for the present study were obtained from the reports on the studies on the western coastal plain of Saudi Arabia by the Saudi Ministry of Water and Electricity (MoWE 2015). Water table measurements were taken from 120 bore wells in the wadi alluvium. The measurements were taken when the water pumps were switched off. Water quality data were obtained from 263 wells. The well locations for the water quality data are shown in Fig. 2. The standard procedure related to water sample collection and analyses was used to obtain the data. The hydrochemical data consist of pH, EC, TDS, Ca, Mg, Na, K, HCO<sub>3</sub>, SO<sub>4</sub>, Cl, NO<sub>3</sub>, Br and SiO<sub>2</sub>.

The data were checked for the accuracy in analysis using the charge balance error (CBE), and all the samples

having CBE of less than 5% were considered for interpretation. Piper plot was prepared using the GW Chart (version 1.29.0.0) developed by the USGS. Graphs for interpreting the ionic relations were prepared in Microsoft Excel. The DEM map and geological map of the area were prepared using ArcGIS 10.3. The piezometric and TDS distribution maps were prepared using SURFER 12. The saturation indices of the principal mineral phases were calculated using the speciation code PHREEQC 2.8.

**Results and discussion**

**General hydrochemistry**

Physiochemical parameters including pH, EC, TDS, major ions, NO<sub>3</sub> and SiO<sub>2</sub> were analyzed for 263 groundwater samples. The general statistics of the analyzed parameters are shown in Table 1. The high standard deviation observed for most of the parameters in the table indicates a wide range of hydrochemical factors influencing the groundwater chemistry. The pH of the analyzed samples ranges from 6.90 to 8.60. Overall the samples are slightly alkaline having a mean pH value of 7.96. The EC ranges

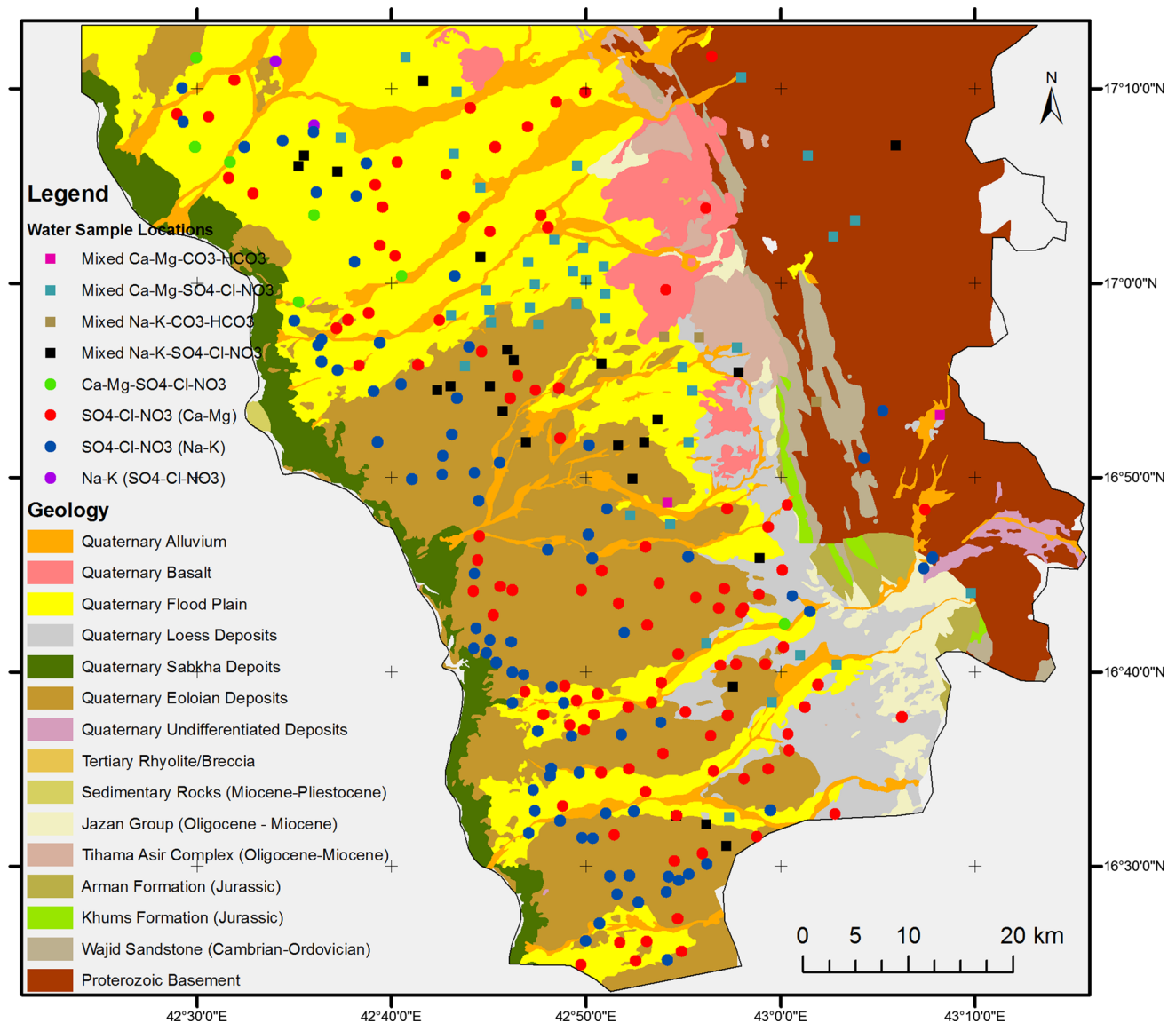


**Fig. 2** Geology and groundwater sample locations. The samples have been classified based on water type as interpreted from Piper plot

from 496 to 13,800  $\mu\text{S}/\text{cm}$  and is related to the TDS of the samples by the relation  $\text{TDS} = 0.7\text{EC}$ .

The TDS values range from 254 to 9603.60 mg/l. Figure 4 shows the TDS distribution map of the study area. A general increase in TDS concentration is observed from the inland toward the coast. According to the Freeze and Cherry (1979) classification, 15.6% of the samples ( $n = 41$ ) fall under the freshwater category with TDS values less than 1000 mg/l. The remaining 84.4% of the samples ( $n = 222$ ) fall under the brackish water category with values ranging between 1000 and 10,000 mg/l. The TDS values show good correlation with Na, Ca, Mg, Cl and  $\text{SO}_4$ .

Na is the most dominant cation (mean: 411.56 mg/l) followed by Ca (mean: 266.30 mg/l), Mg (mean:

86.71 mg/l) and K (mean: 7.08 mg/l). Cl is the most dominant anion (mean: 727.97 mg/l) followed by  $\text{SO}_4$  (mean: 557.73 mg/l) and  $\text{HCO}_3$  (mean: 198.16 mg/l). Natural  $\text{NO}_3$  concentration in groundwater seldom exceeds 10 mg/l. Concentration greater than 10 mg/l is often a consequence of anthropogenic activities such as application of inorganic nitrogenous fertilizers and manures, sewage waste disposal and leakage from septic tanks (Böhlke 2002; WHO 2011; Wu and Sun 2016). The presence of shallow unconfined alluvial aquifer in the study area makes it highly vulnerable to agricultural pollution. The  $\text{NO}_3$  values in the groundwater samples range from 0.02 to 1020 mg/l with an average of 157.80 mg/l. The high values can be attributed to the agricultural practices in the area. Sorghum and millets are the main crops grown in

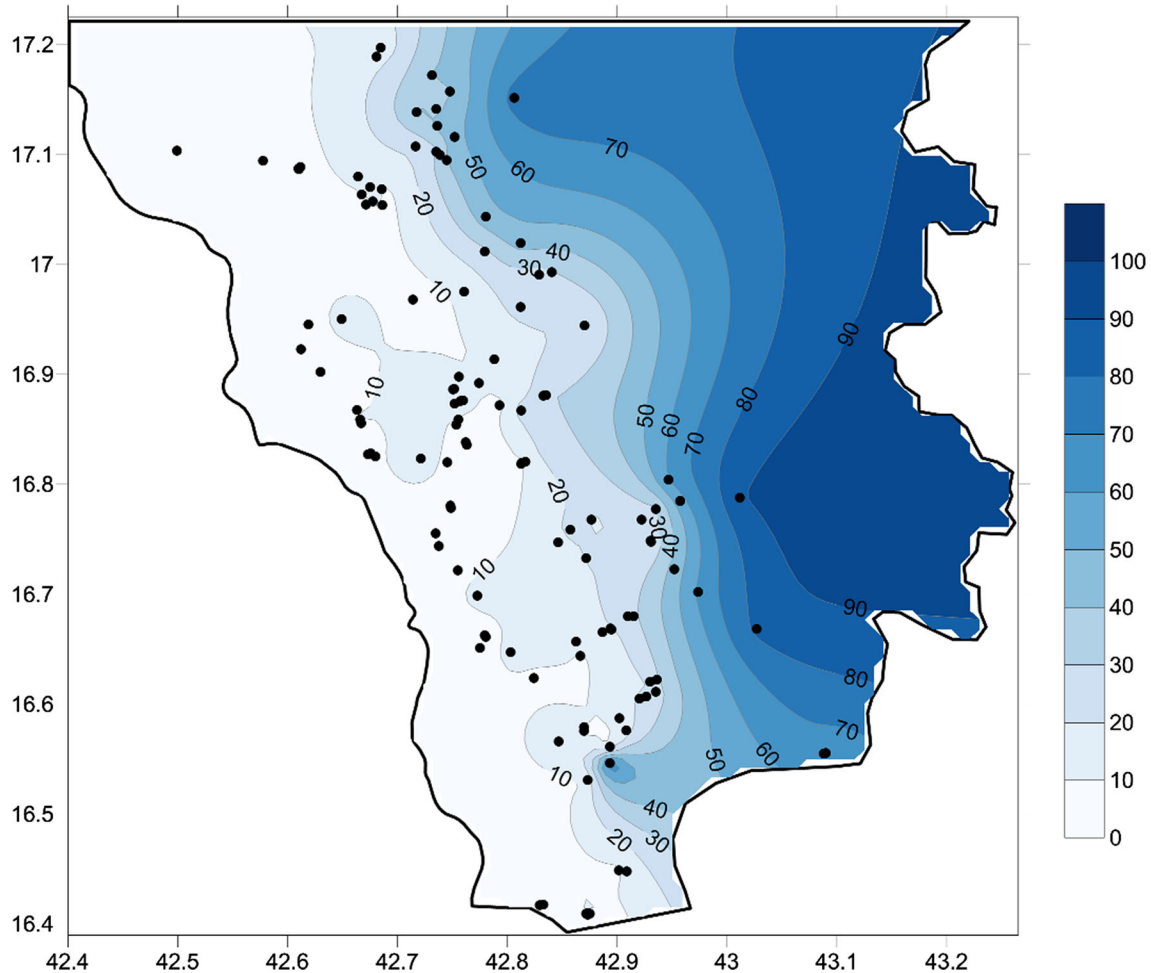


**Fig. 3** Piezometric map of the study area. Black dots represent the locations of water level measurements. All values are in meters above mean sea level

**Table 1** Summary statistics for the analyzed parameters

Parameters	Minimum	Maximum	Mean	SD
pH	6.90	8.60	7.96	0.32
EC	496.00	13,800.00	3704.68	2634.74
TDS	254.80	9603.60	2579.82	1882.99
Ca	21.50	1406.00	266.30	228.56
Mg	6.30	410.00	86.71	70.21
Na	27.30	2098.00	411.56	346.62
K	0.05	85.70	7.08	7.95
HCO <sub>3</sub>	85.00	400.00	198.16	61.20
Cl	17.00	3580.00	727.97	680.94
SO <sub>4</sub>	24.90	2863.00	557.73	527.38
NO <sub>3</sub>	0.02	1020.00	157.80	156.81
SiO <sub>2</sub>	11.10	82.70	41.84	13.26

Electrical conductivity (EC) values are in microsiemens/meter ( $\mu\text{S}/\text{cm}$ ). Total dissolved solids (TDS), major ion and SiO<sub>2</sub> concentrations are given in milligram/liter (mg/l)

the region (FAO 1997). Maize, sesame, tomatoes, egg-plants and melon are other crops and vegetables commonly grown in the area. Since the NO<sub>3</sub> values are much higher than 10 mg/l in most of the sample, it has been included in the major anion category for groundwater facies classification. Figure 5 shows the NO<sub>3</sub> distribution for the study area. The high NO<sub>3</sub> values occur along Quaternary flood plains and eolian deposits where extensive agricultural activities take place.

The SiO<sub>2</sub> values for the groundwater samples ranges from 11.10 to 82.70 mg/l. The presence of SiO<sub>2</sub> in groundwater is primarily attributed to rock–water interaction, and studies have shown the relationship of silica in groundwater with aquifer temperature (Swanberg and Morgan 1978), aquifer lithology (Asano et al. 2003) and aquifer depth (Khan and Umar 2010; Khan et al. 2015). Aquifer lithology and temperature are believed to be the main reason for the presence of high SiO<sub>2</sub> concentrations in

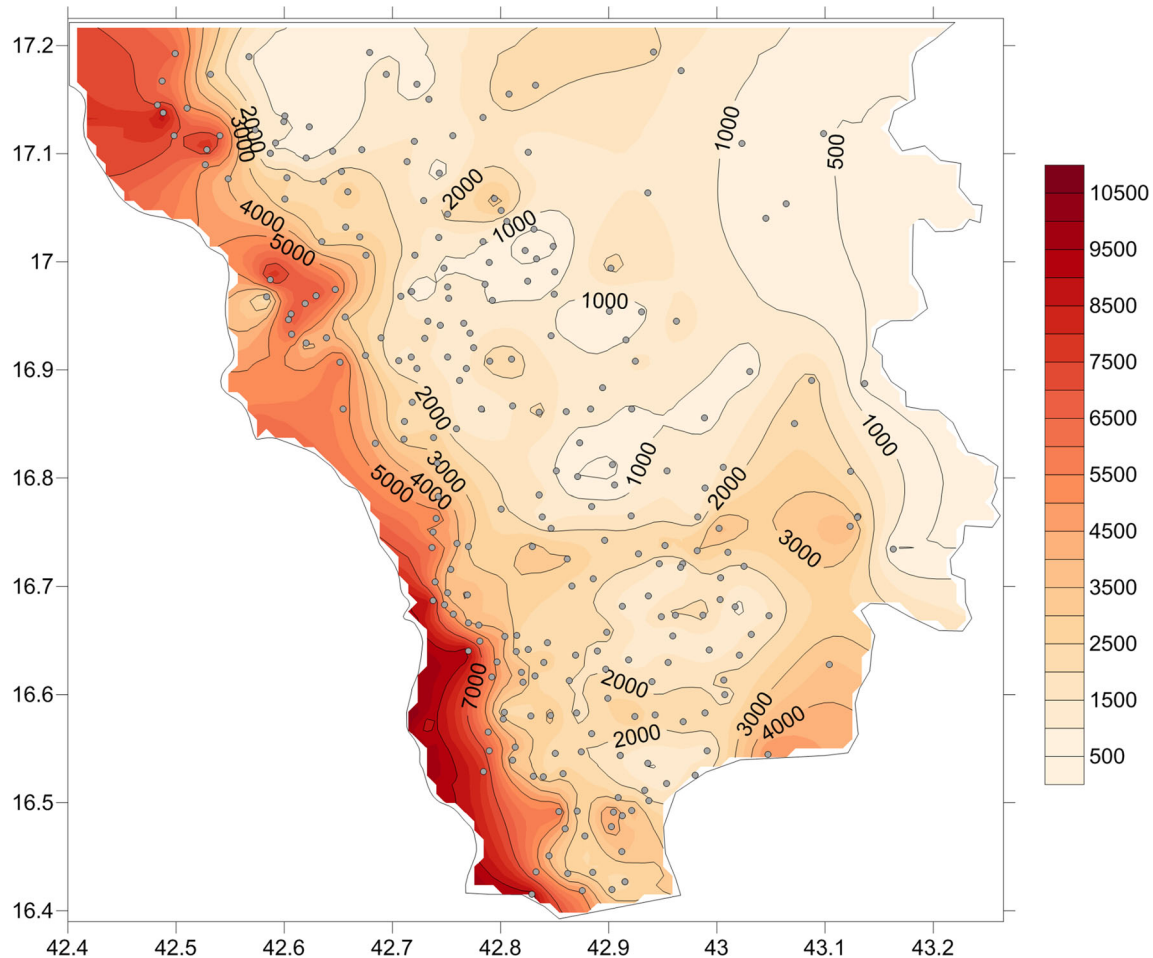


**Fig. 4** TDS distribution map of the study area. All values are in mg/l

the present study (mean: 41.84 mg/l). The standard deviations for all the parameters except pH are very high indicating wide spatial variability of the measured parameters.

### Hydrochemical facies analysis

Groundwater facies classifications for the 263 samples were carried out using the Piper plot. Since  $\text{NO}_3\text{-N}$  values were very high in the groundwater samples (predominantly from agricultural return flow), its concentration was also plotted on the Piper plot together with Cl. The water in the study area can be broadly divided into two categories. Figure 6 shows the classification of the groundwater facies based on the Piper plot, whereas Fig. 2 shows the distribution of the different groundwater facies on the geological map. The first category includes the mixed type of groundwater facies, where there is no clear dominance of any particular ionic species. Sixty-eight groundwater samples belong to this group. The group is characterized by relatively low TDS values which range from 254.8 to

1755.6 mg/l. The average TDS value is 945.7 mg/l. The mixed type of groundwater facies is predominantly confined to the Hijaz–Asir highlands in the eastern part and the north–central part of the study area. The relatively low TDS values of the mixed groundwater facies may be attributed to the rainfall recharge in the highlands and the adjoining areas. It should be mentioned here that typically rainfall recharge is low in hilly regions as the water infiltration capacity is inversely proportional to the slope angle (Daher et al. 2011); however, considering the weathered and fractured nature of the aquifers in such terrains, the groundwater circulation for the minimally infiltrated rainwater is good. The meteoric signature of the groundwater, however, is not very evident on the Piper plot probably due to rock–water interaction. Depending on the dominance of the cations and anions, the mixed type of groundwater facies can be further classified into 4 types, i.e., (a) mixed Ca–Mg– $\text{CO}_3\text{-HCO}_3$  type, (b) mixed Ca–Mg– $\text{SO}_4\text{-Cl-NO}_3$  type, (c) mixed Na–K– $\text{CO}_3\text{-HCO}_3$  type and (d) mixed Na–K– $\text{SO}_4\text{-Cl-NO}_3$  type. The number of samples within each subtype and their average TDS values is mentioned in

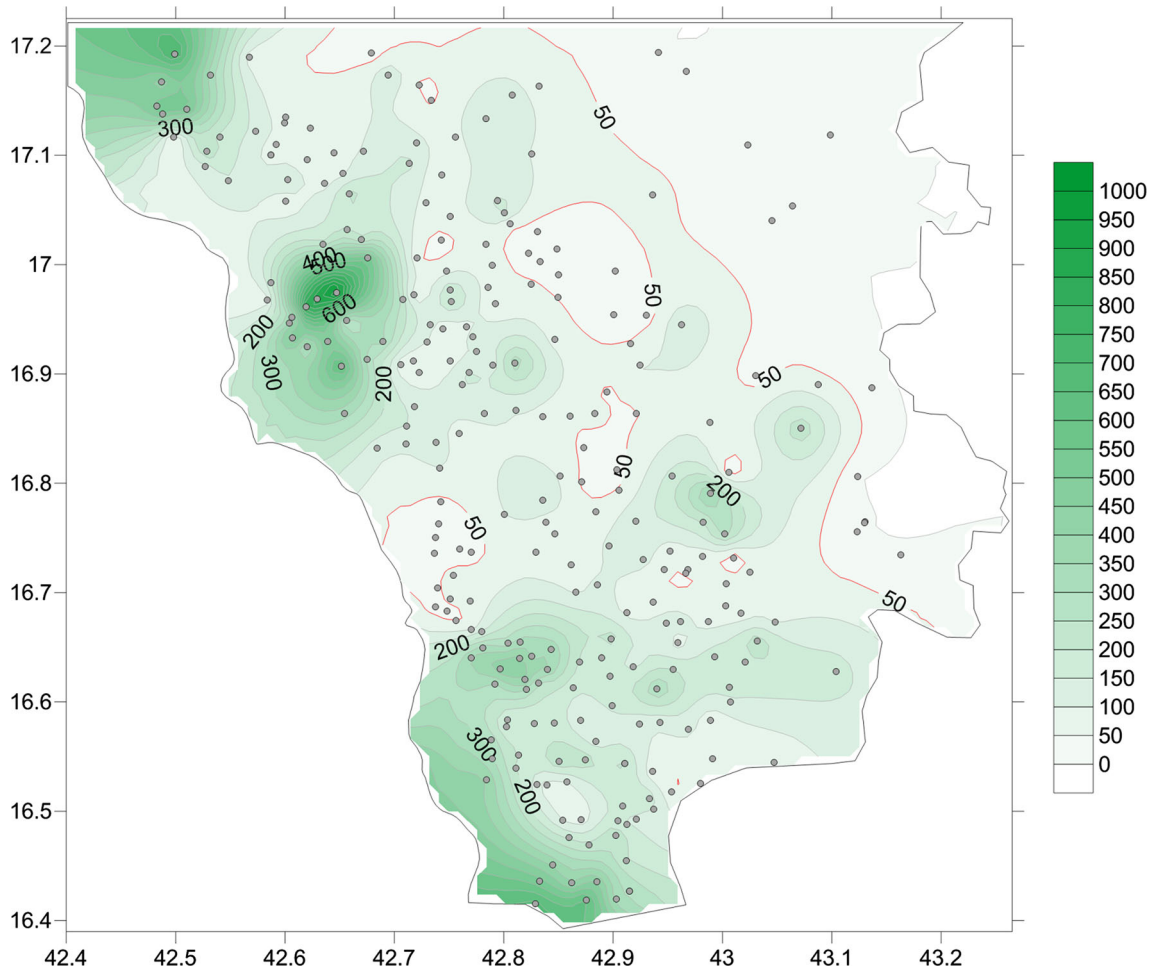


**Fig. 5** NO<sub>3</sub> distribution map of the study area. All values are in mg/l

Table 2. (Ca + Mg)/HCO<sub>3</sub> ratio of less than one is indicative of fresh rainfall recharge or groundwater of meteoric origin (Nazzal et al. 2014). Based on this ratio, 13 samples are indicative of rainfall recharge. Eleven of these samples belong to the mixed groundwater facies and lie close to the elevated zones in the eastern part of the study area.

The second group consisting of 195 water samples belongs to the SO<sub>4</sub>-Cl-NO<sub>3</sub> anionic facies type. This group is characterized by higher values of TDS which range from 723.5 to 9603.6 mg/l. The average TDS value is 3149.7 mg/l (brackish water). The SO<sub>4</sub>-Cl-NO<sub>3</sub> type has been further subdivided into 4 categories, i.e.,

- (a) Ca-Mg-SO<sub>4</sub>-Cl-NO<sub>3</sub> type [more than 80% Ca + Mg and SO<sub>4</sub> + Cl + NO<sub>3</sub>],
- (b) SO<sub>4</sub>-Cl-NO<sub>3</sub> (Ca-Mg) type, [more than 80% SO<sub>4</sub> + Cl + NO<sub>3</sub> and 50–80% Ca + Mg],
- (c) SO<sub>4</sub>-Cl-NO<sub>3</sub> (Na-K) type [more than 80% SO<sub>4</sub> + Cl + NO<sub>3</sub> and 50–80% Na + K] and
- (d) Na-K (SO<sub>4</sub>-Cl-NO<sub>3</sub>) type [more than 80% Na + K and 50–80% SO<sub>4</sub> + Cl + NO<sub>3</sub>].

The SO<sub>4</sub>-Cl-NO<sub>3</sub> (Ca-Mg) and the SO<sub>4</sub>-Cl-NO<sub>3</sub> (Na-K) types of water are the most dominant water type and constitute approximately 71% of the total groundwater samples. Geographically the water samples lying along the coasts are predominantly of the SO<sub>4</sub>-Cl-NO<sub>3</sub> (Na-K) type and are influenced either by the presence of sabkha deposits along the coasts or by saline water intrusion. The average TDS value of this water type is 3506.8 mg/l. The brackish nature of the water in this area can be a result of the dissolution of halite found in the sabkhas or due to the disturbance of the natural saline water-freshwater interface by groundwater pumping which results in up-coning of saline water. The up-coning leads to the mixing of fresh groundwater with seawater and correspondingly high TDS values. The TDS values show an increasing trend from inland toward the coast (Fig. 4).

The Ca-Mg-SO<sub>4</sub>-Cl-NO<sub>3</sub> type of groundwater has the maximum average TDS values. Seven samples belong to this water type. Six of them are in the northwestern part of the study area close to the coast and have TDS values ranging from 2400 to 8330 mg/l and

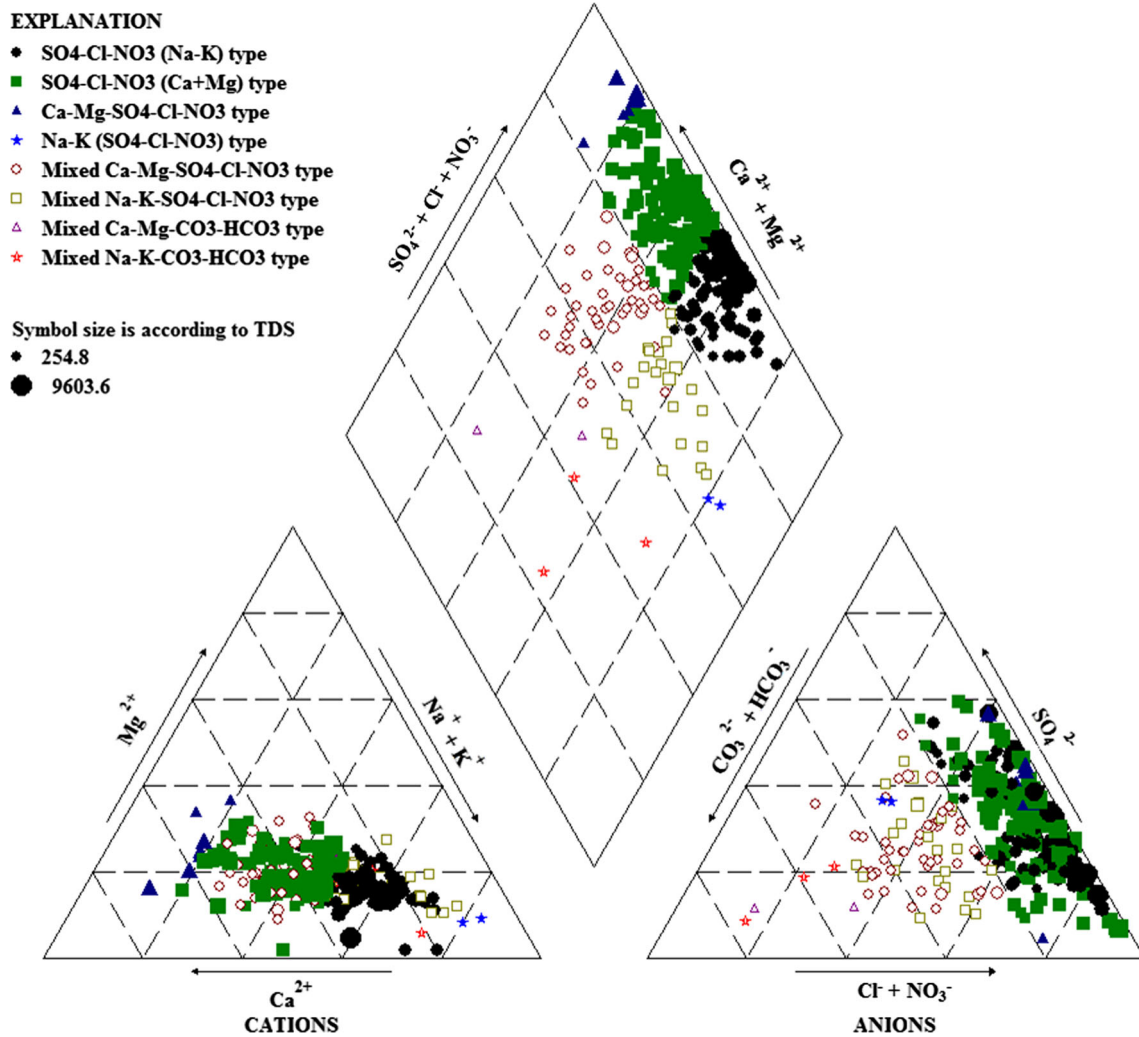


Fig. 6 Piper plot of the groundwater samples

Table 2 Statistics of the number of water samples falling in each type of hydrochemical facies based on Piper plot

Water type	No. of samples	Average TDS (mg/l)	Average NO <sub>3</sub> (mg/l)	Water subtype	No. of samples	Average TDS (mg/l)
Mixed type	68	945.7	65.85	Mixed Ca-Mg-CO <sub>3</sub> -HCO <sub>3</sub>	2	373.9
				Mixed Ca-Mg-SO <sub>4</sub> -Cl-NO <sub>3</sub>	39	914.4
				Mixed Na-K-CO <sub>3</sub> -HCO <sub>3</sub>	3	685
				Mixed Na-K-SO <sub>4</sub> -Cl-NO <sub>3</sub>	24	1076.7
SO <sub>4</sub> -Cl-NO <sub>3</sub> type	195	3149.7	189.86	Ca-Mg-SO <sub>4</sub> -Cl-NO <sub>3</sub>	7	5355
				SO <sub>4</sub> -Cl-NO <sub>3</sub> (Ca-Mg)	103	2756.2
				SO <sub>4</sub> -Cl-NO <sub>3</sub> (Na-K)	83	3506.8
				Na-K (SO <sub>4</sub> -Cl-NO <sub>3</sub> )	2	875.6

are probably influenced by the dissolution of gypsum and halite present in the sabkhas as well as reverse ion exchange. One sample which lies inland in the south-eastern part of the study area has a TDS value of 1807.2 mg/l and appears to be influenced by reverse ion exchange.

The average NO<sub>3</sub> values for the SO<sub>4</sub>-Cl-NO<sub>3</sub> type water are 189.86 mg/l and are clearly influenced by pollution from agricultural sources. Halite dissolution from sabkhas, ion exchange, reverse ion exchange and anthropogenic influences (agricultural pollution) are believed to be the main factors controlling the groundwater chemistry.

### Ionic relationship

#### Na + K versus Cl

The Na + K versus Cl plot (Fig. 7a) shows the possible influence of halite dissolution if the samples plot along the 1:1 equiline (Li et al. 2013). Samples falling on either side of the line shows excessive concentrations and shows secondary bonding affinity (Na with HCO<sub>3</sub> and SO<sub>4</sub>; Cl with Ca and Mg) (Nazzal et al. 2014). Excess concentration of Na points toward ion exchange. Overall there is a dominance of Cl as compared to Na + K. Removal of Na from the groundwater system as a result of reverse ion exchange can be a possible reason for the dominance of Cl.

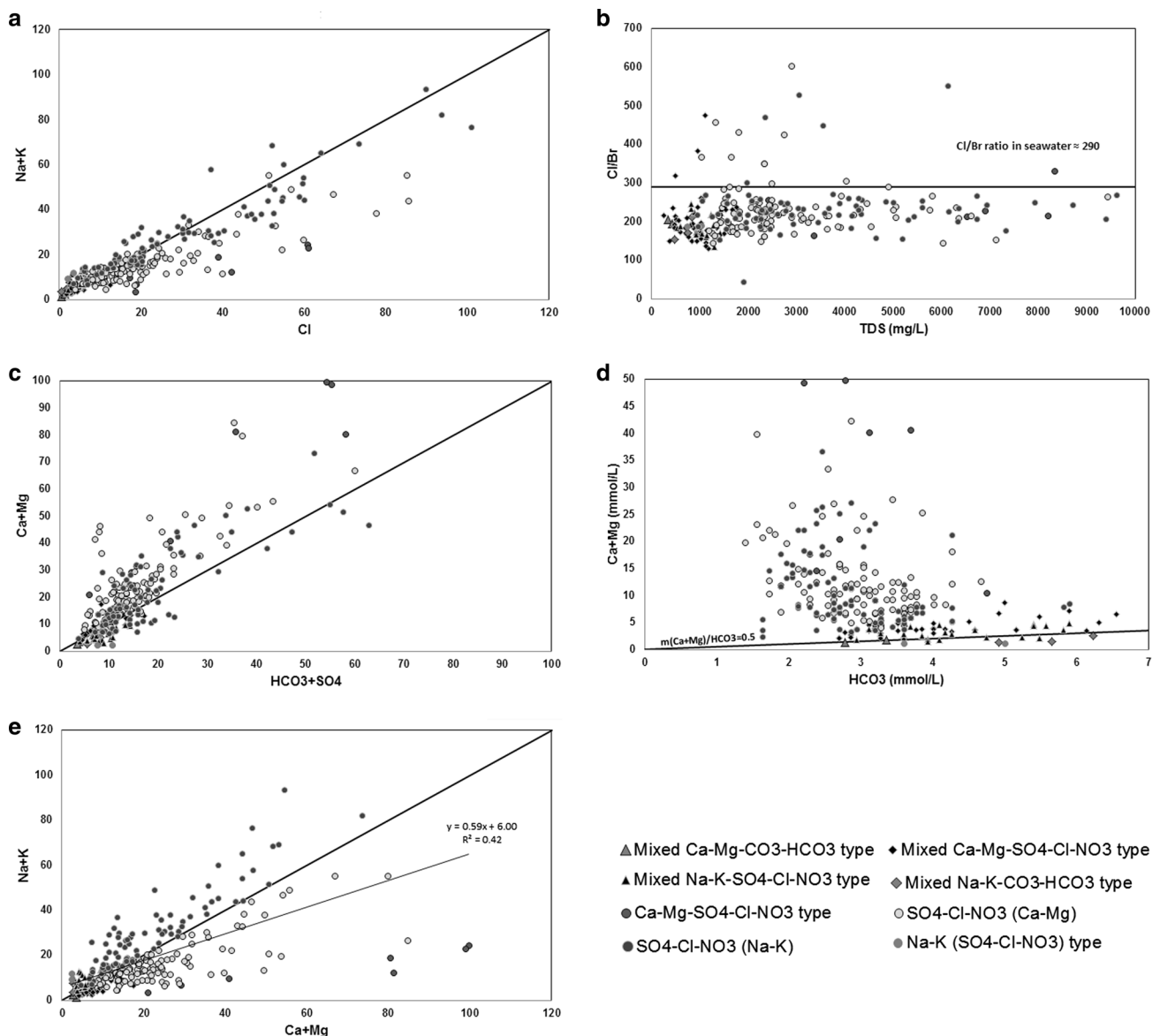


**Fig. 7** Ionic plots **a** Na + K versus Cl, **b** Cl/Br versus TDS, **c** Ca + Mg versus HCO<sub>3</sub> + SO<sub>4</sub>, **d** Ca + Mg versus HCO<sub>3</sub>, **e** Na + K versus Ca + Mg. All values are in meq/l unless otherwise stated

Samples belonging to the  $\text{SO}_4\text{-Cl-NO}_3$  (Ca-Mg) and  $\text{SO}_4\text{-Cl-NO}_3$  (Na-K) type show high concentrations of Na and Cl and are correlated with the high TDS values found in these samples. Higher concentration of chloride in the coastal region due to saline water intrusion has been reported by Singaraja et al. (2014), and its dominance in the present study (average Cl concentration in the  $\text{SO}_4\text{-Cl-NO}_3$  water type is 926.7 mg/l) due to the mixing of saline water and freshwater along the coastal areas cannot be ruled out. The sabkha deposits along the coastal area as shown in the geological map (Fig. 2) can also lead to high Cl concentration due to its interaction with the groundwater. The groundwater levels along the coastal zone as shown in Fig. 3 are very shallow and can easily interact with the sabkha deposits. Anthropogenic pollution (mainly from agricultural activities) can be a possible source of high Cl concentration in groundwater. High Cl values originating from agricultural pollution are doubtful in the present study because of the absence of strong correlation between Cl and  $\text{NO}_3$  values. All the samples belonging to the Ca-Mg- $\text{SO}_4\text{-Cl-NO}_3$  facies are depleted in Na showing the possible influence of reverse ion exchange or the dominance of gypsum dissolution leading to high concentration of Ca and  $\text{SO}_4$ . The excessive Na found in some samples can be a result of the ion exchange reactions or silicate weathering (Li et al. 2016a).

#### Cl/Br ratio

Cl/Br ratio has been frequently used to determine the impact of saline water intrusion in coastal areas. The Cl/Br mass ratio for seawater varies from 288 to 292 (Davis et al. 1998). Rainwater in general has a Cl/Br ratio of less than 200. Cl/Br ratios in potable groundwater show large variation but are generally lower than the ratios found in seawater. Use of NaCl for domestic purposes greatly increases the Cl/Br ratio of groundwater mixed with domestic effluents (Katz et al. 2011). The application of pesticides (methyl bromide) and fertilizers in agricultural farms results in low Cl/Br ratios in water influenced by agricultural return flows (Davis et al. 2001).

The Cl/Br versus TDS plot (Fig. 7b) was investigated in the present study to see the possible influence of saline water intrusion. Overall the samples show a Cl/Br ratio lower than those found in seawater (average ratio for all the samples is 224) with only 7% of the samples (18 samples) showing higher ratios. Ratios higher than the Cl/Br ratio in seawater can probably be the result of halite dissolution. Samples showing Cl/Br ratios higher than those found in seawater are mostly dominated by high Ca concentrations and having average TDS value of 2652 mg/l. Only 3 of the

18 samples showing high Cl/Br ratios have TDS values in excess of 3000 mg/l. All the samples having TDS values of over 3000 mg/l are characterized by an average Cl/Br ratio of 237.6. Based on the Ca + Mg/ $\text{HCO}_3$  ratio, 13 groundwater samples were of meteoric origin. These samples were characterized by average Cl/Br ratio of 183.4. Samples showing  $\text{NO}_3$  values of over 100 mg/l and showing possible influence of agricultural pollution are characterized by an average Cl/Br ratio of 224.7. However, a lack of correlation between Cl, Br and  $\text{NO}_3$  in these samples is indicative of different sources of origin for these ions. No clear evidence of saline water intrusion was found in the present study based on the Cl/Br ratios. The high TDS values along the coastal areas are more influenced by the interaction of groundwater with the sabkhas.

#### Ca + Mg versus $\text{HCO}_3 + \text{SO}_4$

The Ca + Mg versus  $\text{HCO}_3 + \text{SO}_4$  gives an overall idea about calcite/dolomite or gypsum dissolution if samples fall along the 1:1 equiline (Li et al. 2014). Samples falling toward Ca + Mg are indicative of reverse ion exchange, and samples toward  $\text{SO}_4 + \text{HCO}_3$  are indicative of carbonate or silicate weathering (Rajmohan and Elango 2004). In the present study, samples fall on either side of the equiline up to 30 meq/l concentration of Ca + Mg and  $\text{HCO}_3 + \text{SO}_4$  (Fig. 7c). Beyond 30 meq/l concentration, Ca and Mg are dominant in most of samples. Ion exchange or pyrite oxidation in the unsaturated zones (which results in the release of sulfates) may be responsible for higher concentration of  $\text{SO}_4$  in some of the samples. Silicate weathering also results in the points falling toward the  $\text{HCO}_3 + \text{SO}_4$  side. Higher concentrations of Ca and Mg in samples having TDS values of greater than 3000 mg/l may be indicative of mixing between fresh and saline water. This mixing results in reverse ion exchange whereby the Na present in the saline water is replaced by Ca present in the freshwater aquifer matrix. This phenomenon has been reported from groundwaters on the fringe of saline water intrusion (Lloyd and Heathcote 1985). Most of these samples lie along the coastal areas and include the  $\text{SO}_4\text{-Cl-NO}_3$  type of groundwater facies. The molar ratio of Ca + Mg and  $\text{HCO}_3$  was compared (Fig. 7d) to see the influence of silicate weathering. The ratio of  $m(\text{Ca} + \text{Mg})/\text{HCO}_3$  should be close to 0.5 in the presence of weathering of silicate minerals such as pyroxenes and amphiboles (Sami 1992). Samples belonging to the mixed-water facies lie close to this molar ratio and confirm the presence of silicate weathering. In the absence of carbonate-bearing lithology in the study area, the contribution from carbonate weathering can be ruled out.

### *Na + K versus Ca + Mg*

Ionic abundance plot of alkalis (Na + K) versus the alkaline earth elements (Ca + Mg) shows a mixed type of trend with samples falling on either side of the equiline (Fig. 7e). The ion pairs are weakly correlated ( $R^2 = 0.42$ ). As evident from the TDS values and Cl/Br ratios, saline water was not encountered in the area; however, mixing of seawater with the fresh groundwater has been found in the study area. Areas close to the sea coast are characterized by the dominance of Na + K over Ca + Mg and show higher degree halite dissolution. Areas next to this zone and in the central portion of the study area are characterized by the dominance of Ca + Mg over Na + K. This is mainly due to reverse ion exchange which is brought about by the partial mixing of saline water (due to halite dissolution from sabkhas) with the freshwater in the aquifer. Samples showing excessive Na + K further inland might be indicative of silicate weathering or ion exchange.

### Base ion exchange

In case of base ion exchange occurring in groundwater, the excess of Ca and Mg left after bonding with  $\text{SO}_4$  and  $\text{HCO}_3$  is balanced by the excess of Cl left after bonding with Na and K and vice versa (Zaidi et al. 2015). In the present study,  $\text{NO}_3$  values are very high and are also treated as a major ion.  $\text{NO}_3$  shows primary bonding affinity with Na and K and will form  $\text{NaNO}_3$  or  $\text{KNO}_3$  species. Therefore, the plot of  $(\text{Ca} + \text{Mg}) - (\text{SO}_4 + \text{HCO}_3)$  versus  $(\text{Na} + \text{K}) - (\text{Cl} + \text{NO}_3)$  should be a straight line with a slope of  $-1$  and an intercept of 0 if all the Ca, Mg and Na present in the groundwater are taking part in the ion exchange reactions (Li et al. 2016b). The plot (Fig. 8a) shows a slope of  $-1$  and y intercept of 0.56 and a strong correlation of 0.97. This clearly confirms the fact that base ion exchange (reverse ion exchange as well as ion exchange) is occurring in the groundwater of the study area.

The modified Piper diagram (Fig. 8b) proposed by Chadha (1999) was also analyzed to understand the geochemical processes influencing the groundwater chemistry. As expected most of the samples fall within field 6 which is affected by reverse ion exchange and field 7 which is characterized by the presence of brackish water (mainly along the coast). The samples belonging to the mixed groundwater facies (based on Piper classification in Fig. 6) fall close to the origin of the two coordinates with a very few samples representing recharge water and groundwater influenced by ion exchange.

The chloro-alkaline indices, CAI 1 and CAI 2, have been frequently used by numerous workers as it provides a quantitative evidence about cation exchange reactions

(Wang et al. 2015; Li et al. 2016c; Zaidi et al. 2016). It was proposed by Schoeller (1997) and is calculated as:

$$\text{CAI 1} = [\text{Cl} - (\text{Na} + \text{K})]/\text{Cl}$$

and

$$\text{CAI 2} = [\text{Cl} - (\text{Na} + \text{K})]/(\text{Cl} + \text{HCO}_3 + \text{SO}_4 + \text{NO}_3),$$

where all the values are expressed in meq/l. A positive value is indicative of reverse ion exchange whereby the Na + K in groundwater is replaced by Ca + Mg in the aquifer matrix. Figure 8c shows the CAI 1 versus the CAI 2 plot. Evidences of both ion exchange and reverse ion exchange can be seen in the plot. Table 3 shows the average CAI 1 and CAI 2 for the different groundwater facies present in the area. As expected, samples dominated by the presence of Ca and Mg show positive values indicating reverse ion exchange, whereas the mixed groundwater facies and facies dominated by Na + K show ion exchange. The findings are in accordance with the findings of the modified Piper plot.

As evident from the Cl/Br ratios and the salinity values, pure seawater was not found any of the wells. Based on the facies analysis and the location of the facies in the area, it is believed that the  $\text{SO}_4\text{-Cl-NO}_3$  (Na + K) groundwater facies is more influenced by rock-water interaction brought about by halite dissolution rather than saline water intrusion. Moving away from the coast, the  $\text{SO}_4\text{-Cl-NO}_3$  (Ca + Mg) groundwater facies is found which is influenced by reverse ion exchange or reverse softening.

### Silicate weathering

The presence of dissolved silica in the analyzed samples shows the presence of silicate weathering. Since the products of silicate weathering are varied (Das and Kaur 2001), its quantification in the groundwater system is difficult. The plot of Na + K versus the total cations (TZ) is indicative of silicate weathering if the samples fall along the  $\text{Na} + \text{K} = 0.5\text{TZ}$  (Kumar et al. 2009; Srinivasamoorthy et al. 2014) (Fig. 9a). Samples fall along the 0.5TZ line indicating the presence of silicate weathering. Samples falling away from the line and showing low concentrations of Na and K are indicative of reverse ion exchange.

Carbonate weathering does not result in the formation of silica, whereas weathering of silicate minerals such as feldspar releases considerable amount of silica in the groundwater; thus, a comparison between the  $\text{HCO}_3$  and  $\text{SiO}_2$  concentration in groundwater can give an indication of silicate or carbonate weathering (Fig. 9b). Samples falling below the  $\text{HCO}_3 = 5\text{SiO}_2$  is indicative of silicate weathering while those falling above the  $\text{HCO}_3 = 10\text{SiO}_2$  are indicative of carbonate weathering. The coastal plain comprising of eolian deposits and alluvium which serve as

**Fig. 8** Plots showing base ion exchange **a** Ca + Mg–(HCO<sub>3</sub> + SO<sub>4</sub>) versus Na + K–(Cl + NO<sub>3</sub>), **b** modified Piper plot (after Chadha 1999), **c** chloro-alkaline indices (CAIs) for the analyzed samples. All values are in meq/l

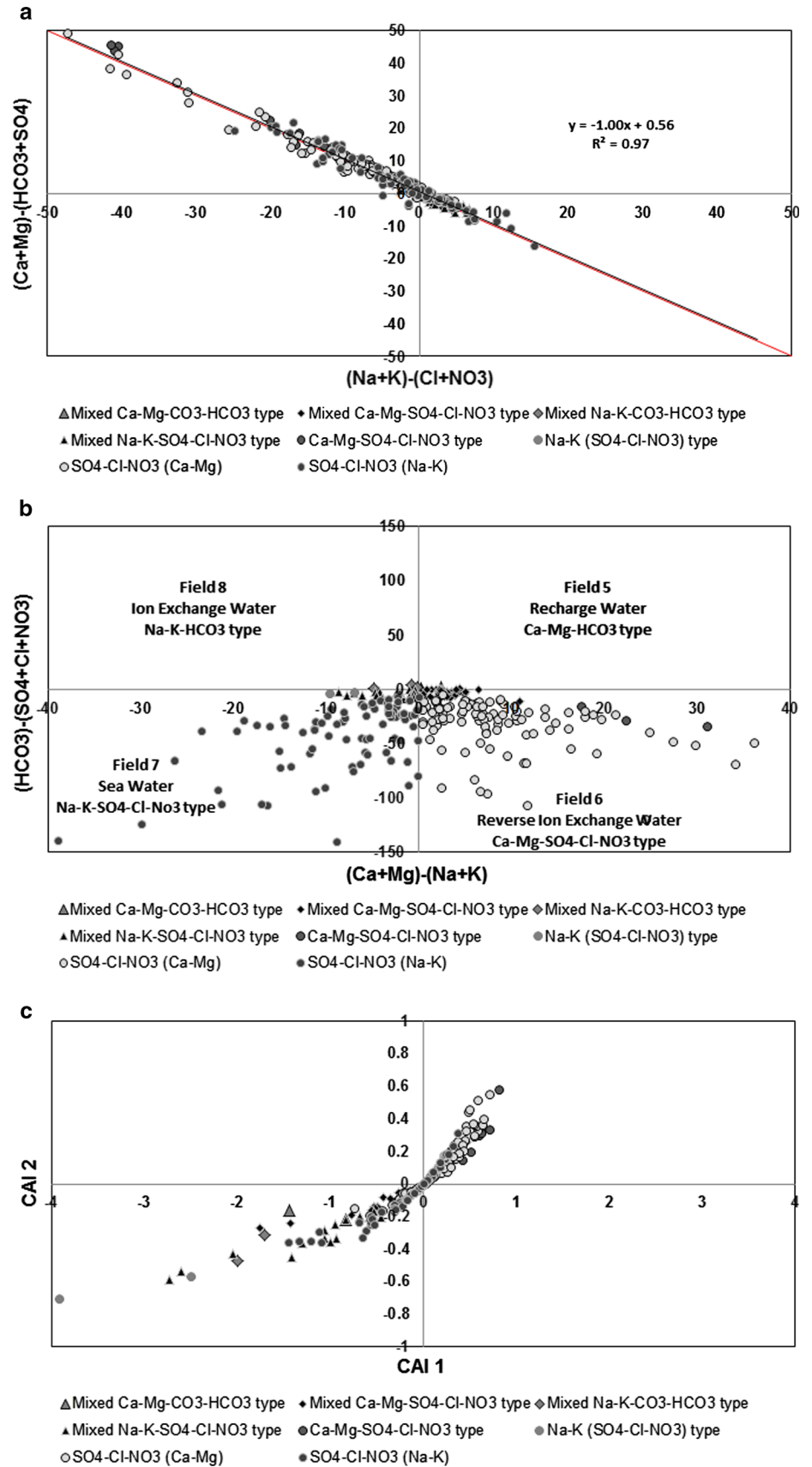


**Table 3** Average values of CAI 1 and CAI 2 for the different water types

Water type	CAI 1	CAI 2
Ca–Mg–SO <sub>4</sub> –Cl–NO <sub>3</sub>	0.6148	0.3202
Mixed Ca–Mg–CO <sub>3</sub> –HCO <sub>3</sub>	–1.1324	–0.1887
Mixed Ca–Mg–SO <sub>4</sub> –Cl–NO <sub>3</sub>	–0.2196	–0.0462
Mixed Na–K–CO <sub>3</sub> –HCO <sub>3</sub>	–3.3331	–0.4149
Mixed Na–K–SO <sub>4</sub> –Cl–NO <sub>3</sub>	–0.8587	–0.2408
Na–K (SO <sub>4</sub> –Cl–NO <sub>3</sub> )	–3.2096	–0.6355
SO <sub>4</sub> –Cl–NO <sub>3</sub> (Ca–Mg)	0.1534	0.1069
SO <sub>4</sub> –Cl–NO <sub>3</sub> (Na–K)	–0.1257	–0.0273

the main aquifer unit in the area comprises of feldspar grains. Feldspar grains are susceptible to weathering and alteration. Their interaction with groundwater has led to silicate weathering. Samples falling along the Na + K = 0.5TZ line in Fig. 10a and showing HCO<sub>3</sub>/SiO<sub>2</sub> ratio of less than 5 (Fig. 10b) are indicative of silicate weathering. However, Fig. 10b shows that samples from groundwater facies dominated by the presence of Ca and Mg show HCO<sub>3</sub>/SiO<sub>2</sub> values of less than 5. The high concentration of SiO<sub>2</sub> in samples dominated by Ca and Mg can be a result of silica/quartz dissolution because other than silicate weathering the dissolution of quartz (also present in the eolian deposits and alluvium) can also be a source of silica in groundwater. Solubility of crystalline silica is small at normal groundwater temperatures but may increase considerably in geothermal waters (Gunnarsson and Arnórsson 2000). The study area has been extensively investigated for geothermal energy resources, and promising results have been obtained (Hussein et al. 2013; Lashin and Al Arifi 2014). In the present study, all the investigated samples have SiO<sub>2</sub> concentration in excess of 50 mg/l and are indicative of silica dissolution by geothermal waters as well.

**Saturation indices**

The groundwater quality in an area is greatly influenced by the presence of different solutes which can be derived from the atmosphere or by the weathering and erosion of rocks and soils (Saleh et al. 1999). The aquifer lithology through which the groundwater flows influences the dominance of a particular ionic species, mainly through rock–water interaction. Under equilibrium conditions, the groundwater is said to be saturated with a given mineral species; however, in nature it is rarely the case. Either the groundwater is undersaturated with respect to a given species and continues to dissolve more minerals through dissolution until it reaches a state of saturation and any further dissolution results in the oversaturation of that particular species. The oversaturated condition finally leads to the precipitation of a given mineral (Deutsch and Siegel 1997). Chemical equilibrium for a particular mineral species can be examined by calculating the saturation index (Li et al. 2010). It is expressed as

$$SI = \log(IAP/KT),$$

where SI is the saturation index of the mineral, IAP is the ion activity product and KT is the solubility constant at temperature *T*. If the water is in thermodynamic equilibrium with a particular mineral species, then SI for that mineral species is 0. An under saturated mineral species in groundwater has a negative SI (<0) and is indicative of dissolution reactions, and a positive SI (>0) indicates the groundwater is oversaturated with respect to that mineral species and will result in precipitation of that mineral (Truesdell and Jones 1974).

Figure 10 shows the SI for the common mineral species found in water versus the TDS. The groundwater of the study area is found to be undersaturated with respect to gypsum, anhydrite and halite. The aquifers are predominantly oversaturated with respect to calcite and dolomite,

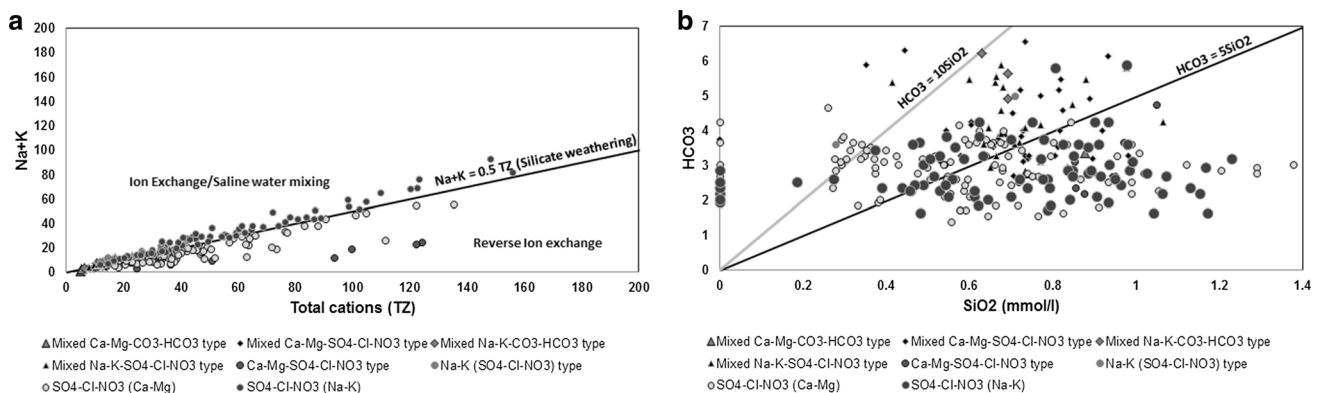


**Fig. 9** Plots showing silicate weathering **a** Na + K versus total cations (TZ), **b** HCO<sub>3</sub> versus SiO<sub>2</sub>. Values are in mg/l unless otherwise stated

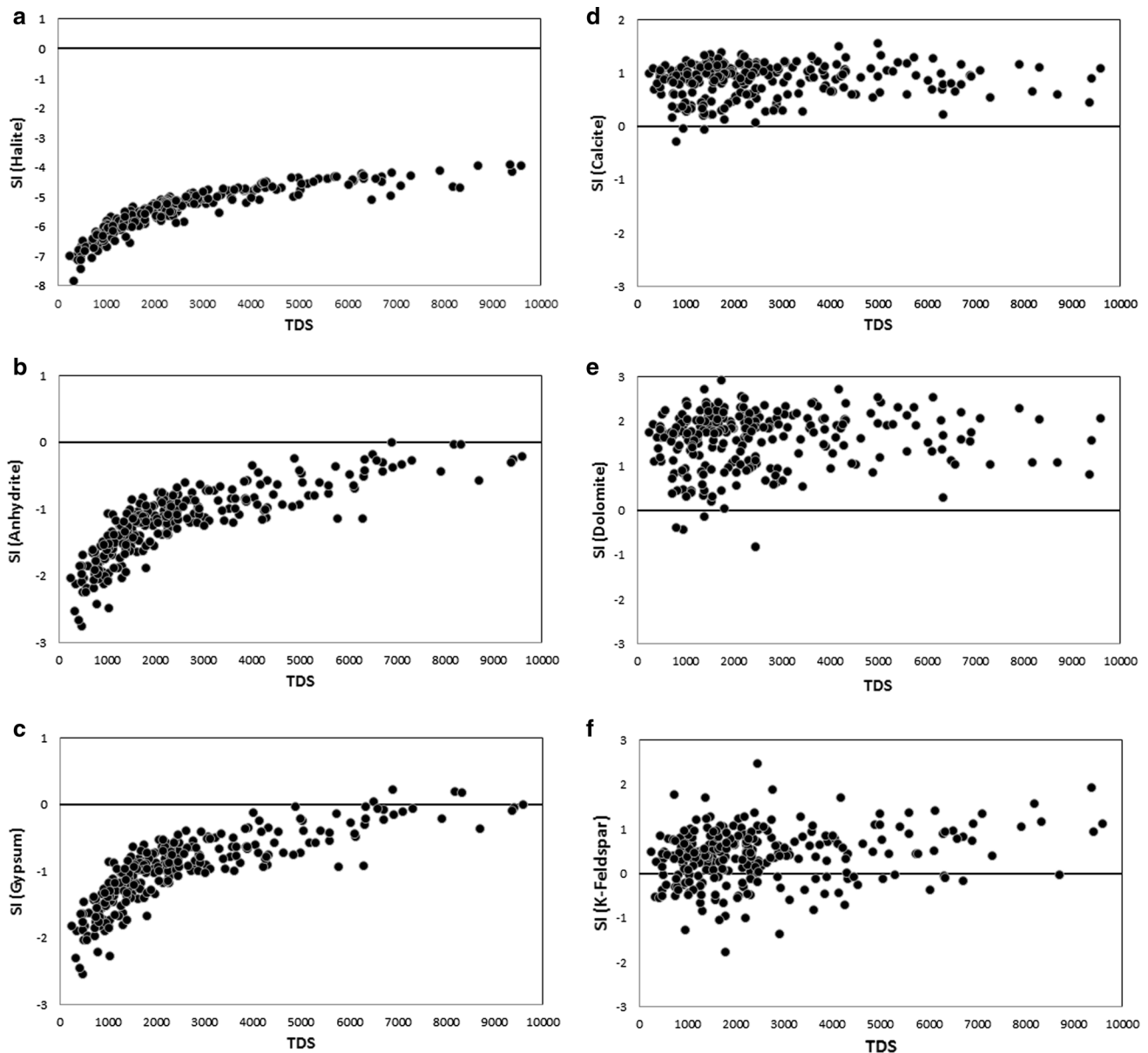


**Fig. 10** Plots showing saturation indices of different mineral species with respect to TDS **a** halite, **b** anhydrite, **c** gypsum, **d** calcite, **e** dolomite, **f** K-feldspar. TDS values are in mg/l

whereas the samples appear to be partially saturated and partially unsaturated with respect to K-feldspars.

Sabkha deposits along the coasts in the study area comprising of gypsum and halite are responsible for their dissolution. Gypsum, halite and anhydrite dissolution also shows a strong correlation with the TDS values indicating increasing saturation of these minerals with increasing TDS. The TDS map in Fig. 4 shows a general increase in TDS concentration from the inland toward the coastal area, and this increase is mainly due to the presence of ionic species such as Ca, Na,  $\text{SO}_4$  and Cl.

Calcite and dolomite show oversaturated conditions; however, the absence of carbonate-bearing lithology does

not support the obtained results from speciation analysis. Silicate weathering in the central and eastern part of the study area is also confirmed by the speciation analysis where some groundwater samples appear undersaturated with respect to K-feldspars and are responsible for silicate dissolution/weathering. As mentioned in the hydrogeology section, the unconfined alluvial/coastal sediments form the main aquifer unit in the study area. K-feldspars frequently constitute the sand grains found in alluvial aquifers and are one of the sources of dissolved silica in the region. However, the K-feldspar dissolution does not show any correlation with the TDS values indicating that they are not an important factor contributing to the TDS in groundwater.

## Conclusions

The present study for assessing the groundwater chemistry in the Tihama coastal plains in parts of the Jazan Province using hydrochemical data suggests mineral dissolution as a result of rock–water interaction and anthropogenic influences as the main source of various ions in groundwater. Na, Cl, Ca and SO<sub>4</sub> were found to be the major ions contributing to the bulk of the TDS. The TDS shows a wide range varying from 250 mg/l along the eastern highlands and central portion of the study area to as high as 9600 mg/l along the coast. High TDS values along the coast are attributed to the dissolution of gypsum and halite found in the sabkha deposits.

SO<sub>4</sub>–Cl–NO<sub>3</sub> groundwater facies is the dominating groundwater facies in the area. The central portion of the study area is dominated by the presence of SO<sub>4</sub>–Cl–NO<sub>3</sub> (Ca–Mg) type of groundwater facies and is influenced by reverse ion exchange. Reverse ion exchange reactions are also evident in the modified Piper plot and chloro-alkaline indices. Chloro-alkaline indices also show the presence of ion exchange in the mixed groundwater facies and facies dominated by Na + K. Groundwater facies showing the clear presence of meteoric groundwater sources is absent in the regions; however, ionic relationships between Ca + Mg and HCO<sub>3</sub> indicate the presence of rainfall recharge in the eastern part of the study.

The coastal aquifer comprising of alluvial sand grains also indicates the presence of silicate weathering as evident from the Na + K versus total cation plots and HCO<sub>3</sub> versus SiO<sub>2</sub> ratios. High average silica values (mean of approximately 42 mg/l) are also attributed to the silica dissolution process in geothermal water found in the region.

The Cl/Br ratios in the investigated groundwater samples are much less than those found in seawater and are not indicative of saline water intrusion and mostly point toward the use of bromide-bearing fertilizers used for agricultural production. The elevated NO<sub>3</sub> concentration has also been attributed to agricultural activities though a lack of correlation between Br and NO<sub>3</sub> indicates different sources for the two ions.

Though the presence of brackish groundwater in the study area is primarily attributed to the interaction of groundwater with the salt flats, judicious groundwater pumping in the region is advised to prevent saline water intrusion. Safe agricultural practices are also advised to prevent the extent of agricultural pollution which otherwise may have adverse effects on human health if consumed through the public supply wells.

**Acknowledgements** The authors would like to extend their sincere appreciation to the Deanship of Scientific Research at King Saud

University for its funding of this research through the Research Group Project No. RGP-VPP-230.

## References

- Abdalla F (2016) Ionic ratios as tracers to assess seawater intrusion and to identify salinity sources in Jazan coastal aquifer, Saudi Arabia. *Arab J Geosci* 9(1):1–12
- Abdalla F, Al-Turki A, Al Amri A (2015) Evaluation of groundwater resources in the Southern Tihama plain, Saudi Arabia. *Arab J Geosci* 8(5):3299–3310
- Al-Ahmadi ME, El-Fiky AA (2009) Hydrogeochemical evaluation of shallow alluvial aquifer of Wadi Marwani, western Saudi Arabia. *J King Saud Univ Sci* 21(3):179–190
- Al-Bassam AM, Hussein MT (2008) Combined geo-electrical and hydro-chemical methods to detect salt-water intrusion: a case study from southwest Saudi Arabia. *Manag Environ Qual Int J* 19(2):179–193
- Asano Y, Uchida T, Ohte N (2003) Hydrologic and geochemical influences on the dissolved silica concentration in natural water in a steep headwater catchment. *Geochim Cosmochim Acta* 67(11):1973–1989
- Batayneh A, Elawadi E, Mogren S, Ibrahim E, Qaisy S (2012) Groundwater quality of the shallow alluvial aquifer of wadi Jazan (southwest Saudi Arabia) and its suitability for domestic and irrigation purpose. *Sci Res Essays* 7(3):352–364
- Böhlke JK (2002) Groundwater recharge and agricultural contamination. *Hydrogeol J* 10(1):153–179
- Chadha DK (1999) A proposed new diagram for geochemical classification of natural waters and interpretation of chemical data. *Hydrogeol J* 7(5):431–439
- Dabbagh ME, Rogers JJ (1983) Depositional environments and tectonic significance of the Wajid Sandstone of southern Saudi Arabia. *J Afr Earth Sci* 1(1):47–57
- Daher W, Pistre S, Kneppers A, Bakalowicz M, Najem W (2011) Karst and artificial recharge: theoretical and practical problems. *J Hydrol* 408:189–202
- Das BK, Kaur P (2001) Major ion chemistry of Renuka lake and weathering processes, Sirmour district, Himachal Pradesh, India. *Environ Geol* 40(7):908–917
- Davis SN, Whittemore DO, Fabryka-Martin J (1998) Uses of chloride/bromide ratios in studies of potable water. *Ground Water* 36(2):338–350
- Davis SN, Cecil LD, Zreda M, Moysey S (2001) Chlorine-36, bromide, and the origin of spring water. *Chem Geol* 179(1):3–16
- Deutsch WJ, Siegel R (1997) Groundwater geochemistry: fundamentals and applications to contamination. CRC Press, Boca Raton
- El Alfy M, Lashin A, Al-Arifi N, Al-Bassam A (2015) Groundwater characteristics and pollution assessment using integrated hydro-chemical investigations and multivariate geostatistical techniques in arid areas. *Water Resour Manag* 29(15):5593–5612
- Fairer GM (1983) Reconnaissance geologic map of the Sabya quadrangle, sheet 17/42D, Kingdom of Saudi Arabia. DMMR geoscience map GM-69
- FAO (1997) Agriculture and consumer protection, plant nematode problems and their control in the Near East region. FAO Cooperate Document Repository. <http://www.fao.org/docrep/v9978e/v9978e0k.htm>. Accessed 27 Apr 2017
- Freeze RA, Cherry JA (1979) Groundwater: Prentice Hall. Englewood Cliffs, New Jersey
- Gunnarsson I, Arnórsson S (2000) Amorphous silica solubility and the thermodynamic properties of H<sub>4</sub>SiO<sub>4</sub> in the range of 0 to 350 C at P sat. *Geochim Cosmochim Acta* 64(13):2295–2307

- Hussein MT, Ibrahim KE (1997) Electrical resistivity, geochemical and hydrogeological properties of wadi deposits, Western Saudi Arabia. *J King Abdul Aziz Univ* 9(1):55–72
- Hussein MT, Lashin A, Al Bassam A, Al Arifi N, Al Zahrani I (2013) Geothermal power potential at the western coastal part of Saudi Arabia. *Renew Sustain Energy Rev* 26:668–684
- Katz BG, Eberts SM, Kauffman LJ (2011) Using Cl/Br ratios and other indicators to assess potential impacts on groundwater quality from septic systems: a review and examples from principal aquifers in the United States. *J Hydrol* 397(3):151–166
- Khan MMA, Umar R (2010) Significance of silica analysis in groundwater in parts of Central Ganga Plain, Uttar Pradesh, India. *Curr Sci* 98(9):1237–1240
- Khan A, Umar R, Khan HH (2015) Significance of silica in identifying the processes affecting groundwater chemistry in parts of Kali watershed, Central Ganga Plain, India. *Appl Water Sci* 5(1):65–72
- Kumar M, Kumari K, Singh UK, Ramanathan AL (2009) Hydrogeochemical processes in the groundwater environment of Muktsar, Punjab: conventional graphical and multivariate statistical approach. *Environ Geol* 57(4):873–884
- Lashin A, Al Arifi N (2014) Geothermal energy potential of southwestern of Saudi Arabia “exploration and possible power generation”: a case study at Al Khouba area–Jizan. *Renew Sustain Energy Rev* 30:771–789
- Li P-Y, Qian H, Wu J-H, Ding J (2010) Geochemical modeling of groundwater in southern plain area of Pengyang County, Ningxia, China. *Water Sci Eng* 3(3):282–291. doi:10.3882/j.issn.1674-2370.2010.03.004
- Li P, Wu J, Qian H (2013) Assessment of groundwater quality for irrigation purposes and identification of hydrogeochemical evolution mechanisms in Pengyang County, China. *Environ Earth Sci* 69(7):2211–2225. doi:10.1007/s12665-012-2049-5
- Li P, Wu J, Qian H (2014) Origin and assessment of groundwater pollution and associated health risk: a case study in an industrial park, northwest China. *Environ Geochem Health* 36(4):693–712. doi:10.1007/s10653-013-9590-3
- Li P, Wu J, Qian H, Zhang Y, Yang N, Jing L, Yu P (2016a) Hydrogeochemical characterization of groundwater in and around a wastewater irrigated forest in the southeastern edge of the Tengger Desert, Northwest China. *Expo Health* 8(3):331–348. doi:10.1007/s12403-016-0193-y
- Li P, Wu J, Qian H (2016b) Hydrochemical appraisal of groundwater quality for drinking and irrigation purposes and the major influencing factors: a case study in and around Hua County, China. *Arab J Geosci* 9(1):15. doi:10.1007/s12517-015-2059-1
- Li P, Zhang Y, Yang N, Jing L, Yu P (2016c) Major ion chemistry and quality assessment of groundwater in and around a mountainous tourist town of China. *Expo Health* 8(2):239–252
- Lloyd JW, Heathcote JAA (1985) Natural inorganic hydrochemistry in relation to ground water. Clarendon Press, Oxford
- Mogren S, Batayneh A, Elawadi E, Al-Bassam A, Ibrahim E, Qaisy S (2011) Aquifer boundaries explored by geoelectrical measurements in the Red Sea coastal plain of Jazan area, Southwest Saudi Arabia. *Int J Phys Sci* 6(15):3688–3696
- MoWE (2015) Detailed water resources studies of the western coastal plain of Saudi Arabia. Ministry of Water and Electricity, Kingdom of Saudi Arabia. Unpublished report
- Nazzal Y, Ahmed I, Al-Arifi NS, Ghrefat H, Zaidi FK, El-Waheidi MM, Batayneh A, Zumlot T (2014) A pragmatic approach to study the groundwater quality suitability for domestic and agricultural usage, Saq aquifer, northwest of Saudi Arabia. *Environ Monit Assess* 186(8):4655–4667
- NCAO (2008) National Center for Atmospheric Research: improve understanding of the atmosphere, earth system, and sun. Annual report, Research application Laboratory. [http://www.nar.ucar.edu/2008/RAL/goal\\_1/priority\\_2.php](http://www.nar.ucar.edu/2008/RAL/goal_1/priority_2.php)
- Rajmohan N, Elango L (2004) Identification and evolution of hydrogeochemical processes in the groundwater environment in an area of the Palar and Cheyyar River Basins, Southern India. *Environ Geol* 46(1):47–61
- Saleh A, Al-Ruwaih F, Shehata M (1999) Hydrogeochemical processes operating within the main aquifers of Kuwait. *J Arid Environ* 42(3):195–209
- Sami K (1992) Recharge mechanisms and geochemical processes in a semi-arid sedimentary basin, Eastern Cape, South Africa. *J Hydrol* 139(1–4):27–48
- Schoeller H (1997) Geochemistry of groundwater. In: *Groundwater studies—an international guide for research and practice*, Chap 15. UNESCO, Paris, pp 1–18
- Sekovski I, Newton A, Dennison WC (2012) Megacities in the coastal zone: using a driver-pressure-state-impact-response framework to address complex environmental problems. *Estuar Coast Shelf Sci* 96:48–59
- Singaraja C, Chidambaram S, Prasanna MV, Thivya C, Thilagavathi R (2014) Statistical analysis of the hydrogeochemical evolution of groundwater in hard rock coastal aquifers of Thoothukudi district in Tamil Nadu, India. *Environ Earth Sci* 71(1):451–464
- Small C, Nicholls RJ (2003) A global analysis of human settlement in coastal zones. *J Coast Res* 19(3):584–599
- Srinivasamoorthy K, Gopinath M, Chidambaram S, Vasanthavigar M, Sarma VS (2014) Hydrochemical characterization and quality appraisal of groundwater from Pungar sub basin, Tamilnadu, India. *J King Saud Univ Sci* 26(1):37–52
- Subyani AM (2004) Geostatistical study of annual and seasonal mean rainfall patterns in southwest Saudi Arabia/Distribution géostatistique de la pluie moyenne annuelle et saisonnière dans le Sud-Ouest de l’Arabie Saoudite. *Hydrol Sci J* 49(5):803–817
- Swanberg CA, Morgan P (1978) The linear relation between temperatures based on the silica content of groundwater and regional heat flow: a new heat flow map of the United States. *Pure Appl Geophys* 117(1–2):227–241
- Taylor RG, Scanlon B, Döll P, Rodell M, Van Beek R, Wada Y, Longuevergne L, Leblanc M, Famiglietti JS, Edmunds M, Konikow L (2013) Ground water and climate change. *Nat Climate Change* 3(4):322–329
- Truesdell AH, Jones BF (1974) WATEQ, a computer program for calculating chemical equilibria of natural waters. *J Res US Geol Surv* 2(2):233–248
- Wang H, Jiang XW, Wan L, Han G, Guo H (2015) Hydrogeochemical characterization of groundwater flow systems in the discharge area of a river basin. *J Hydrol* 527:433–441
- WHO (2011) Guidelines for drinking-water quality, 4th edn. Geneva, Switzerland
- Wu J, Sun Z (2016) Evaluation of shallow groundwater contamination and associated human health risk in an alluvial plain impacted by agricultural and industrial activities, mid-west China. *Expo Health* 8(3):311–329. doi:10.1007/s12403-015-0170-x
- Zaidi FK, Nazzal Y, Jafri MK, Naem M, Ahmed I (2015) Reverse ion exchange as a major process controlling the groundwater chemistry in an arid environment: a case study from northwestern Saudi Arabia. *Environ Monit Assess* 187(10):607
- Zaidi FK, Mogren S, Mukhopadhyay M, Ibrahim E (2016) Evaluation of groundwater chemistry and its impact on drinking and irrigation water quality in the eastern part of the Central Arabian graben and trough system, Saudi Arabia. *J Afr Earth Sci* 120:208–219